

SIMULATION AND EXPERIMENTS OF MULTI-LAYER DRY CASK SHIELDING MATERIALS

Sean Kerrigan, Zeinab Alsmadi, Zainab Alnoamani, Daniel Moneghan, Mohamed Bourham

Department of Nuclear Engineering, North Carolina State University, Raleigh, NC, USA
 (spkerrig@ncsu.edu)

ABSTRACT

The demand for radiation shielding studies has grown with the increasing utilization of radioactive materials. A variety of locations such as nuclear reactors, medical centers, forensic laboratories, nuclear research centers, and nuclear waste storage facilities are potential exposure sites of not only gamma rays but also neutron and/or charged particles. This research investigates the concept of a dry cask with multi-layer shielding and evaluation for high burnup spent fuel storage by using MicroShield as deterministic code. The materials selected as a central theme for dosimetric assessment, are Stainless Steel 304 and 316; and carbon steel. Previously investigated work on glass oxides and concrete forms suggested the utilization of specific forms of glasses and concretes for the multi-layered cask. Conducted gamma ray attenuation experiments compares favorably to MicroShield modeling. Coated samples have shown minimal to nil corrosion rates.

INTRODUCTION

Spent nuclear fuel is stored primarily within dry casks, which involves a stainless steel canister surrounded by concrete over pack. A schematic of a traditional dry cask is shown in Figure 1. The termination of the Yucca Mountain nuclear waste repository has changed the long-term storage plan of spent nuclear fuel. Dry casks storage will continue to be stored at nuclear utilities sites located outside of nuclear power plants. As this storage method involves the dry casks being permanently located in their storage units for up to 300 years, the integrity of the dry cask storage materials must maintain their integrity over this lifetime.

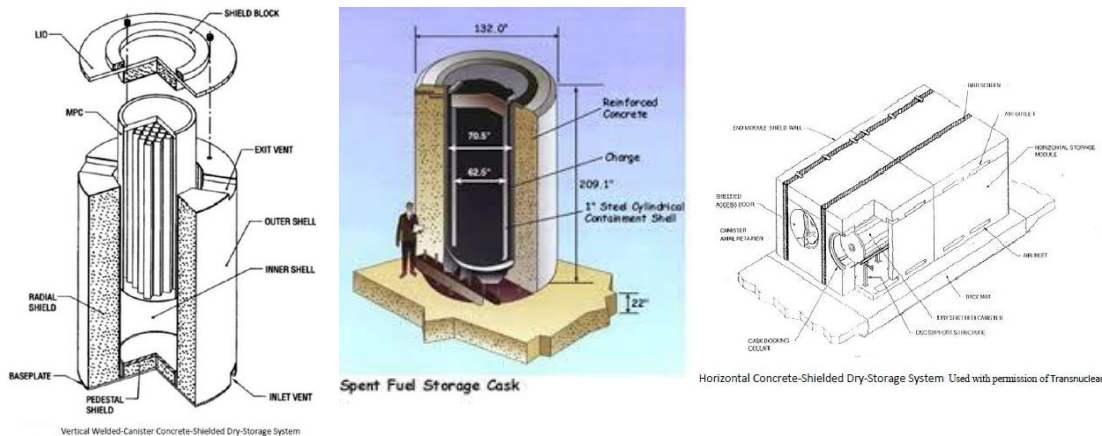


Figure 1. Schematic of the dry cask storage method in both horizontal and vertical orientations retrieved from NRC illustration.

MATERIALS & METHODS

Dry casks are typically made of both 304 and 316 stainless steels. In order to improve the lifetime of the dry cask storage method, a multilayer coating will be added to the surface of the stainless steel canisters as shown in Figure 2. Stainless steel 1" diameter puck substrates are coated with single layers using Physical Vapor Deposition (PVD) in order to study the individual layer performance prior to multilayer analysis.

The multilayer coating involves an external layer of MoS₂ which serves as a solid lubricant as shown by Singh et al. (2015) to improve the handling and transportation of dry casks in order to prevent the formation of micro cracks. The middle layer is formed using a tri-oxide layer known as zirconolite, which serves to improve the corrosion resistance of the steel substrate as corrosion is one of the primary mechanisms of material failure as seen by TiO₂ thin films by Shan et al. (2008). The inner layer of TiN acts as a diffusional barrier, preventing interaction between the multilayer coatings and the underlying stainless steel as observed by Kwon et al. (2006). The longevity of the dry cask storage method requires the integrity of the steel waste package wall and the concrete overpack to be maintained for 300 years. The gamma attenuation and corrosion performance of these materials are investigated.

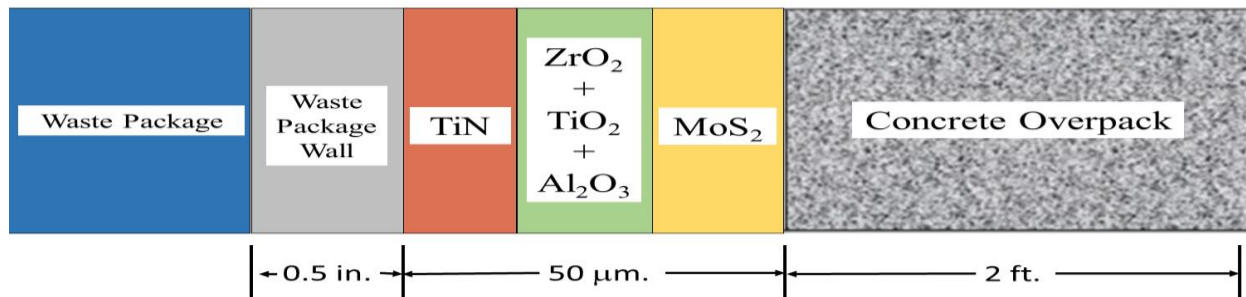


Figure 2. Shielding barriers surrounding the nuclear waste package.

Gamma Attenuation

The attenuation of gamma rays is tested both experimentally and modelled in MicroShield using single layer coated stainless steel samples and concrete overpack of various compositions. The gamma attenuation experimental setup is shown in Figure 3 below. Sources being used include, Cs-137, Ba-133, and three Co-60.

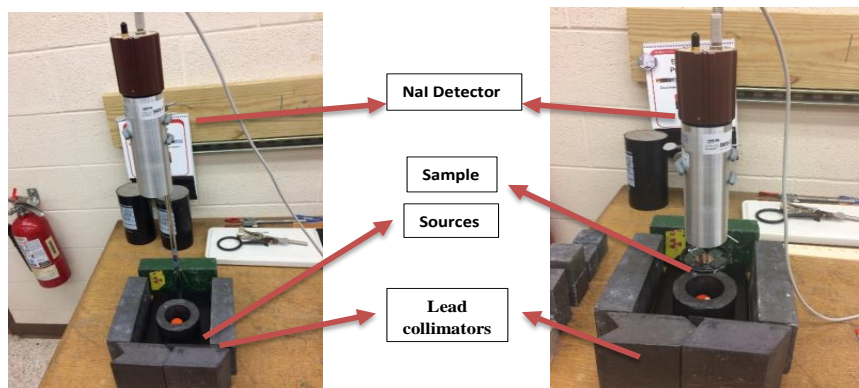


Figure 3. Gamma attenuation experimental setup.

The gamma ray attenuation is performed by measuring the fractional radiation intensity, labelled as I below, compared to the radiation source intensity, labelled as I_0 below. The thickness of each individual sample, labelled as x below, is measured and input into the exponential law in order to obtain the attenuation coefficient:

$$I = I_0 e^{-\mu x} \quad (1)$$

Computational analysis is performed using MicroShield version 9.05 package and Serpent in order to calculate the attenuation coefficient and half value layer (HVL) depending on material density and composition. Dry cask configurations of multi-layered concentric cask designs containing a special inner glass-oxide layer are used as shown in Figure 4. The computational results are compared to experimental results for single layer coated steel substrates.

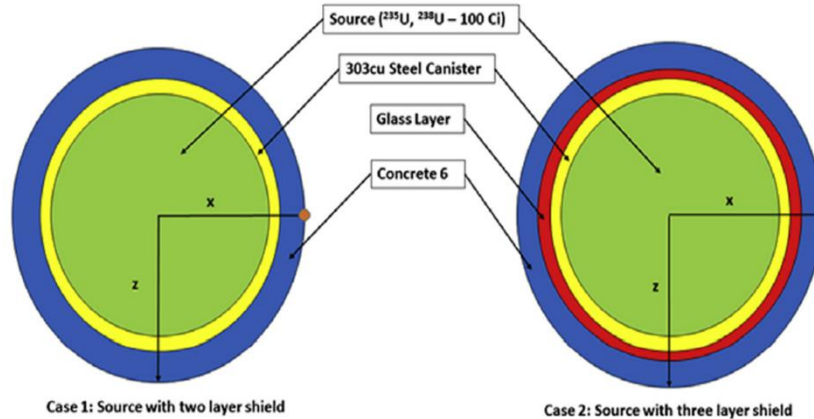


Figure 4. Computational configuration of modelled dry cask using various sources and shielding layers.

Corrosion Testing

Coated single layer steel substrates are placed within a salt-brine circulator using a pH of 5.8 for 40 days to analyse the corrosion effects to the material over this time frame. The salt-brine circulator is shown in Figure 5. A steel substrate sample is placed within the circulator for long periods of time in order to determine the long-term material degradation due to corrosion. Sample mass measurements are taken daily over the course of the experiment.



Figure 5. Salt-brine circulator system for corrosion testing.

RESULTS & DISCUSSION

The linear attenuation of coated steel substrates and concrete samples of various compositions is determined both experimentally and computationally. The experimental setup on the coated steel substrates use Cs-137, Ba-133, and three Co-60 sources while the concrete testing additionally adds three low-energy Cd-109 sources.

Experiments and Modelling on Coated Materials

The effect of adding coatings to stainless steel substrates is shown in Figure 6 & 7 where samples coated with different single and double layered coatings decrease the linear attenuation coefficient between 302 keV to 356 keV.

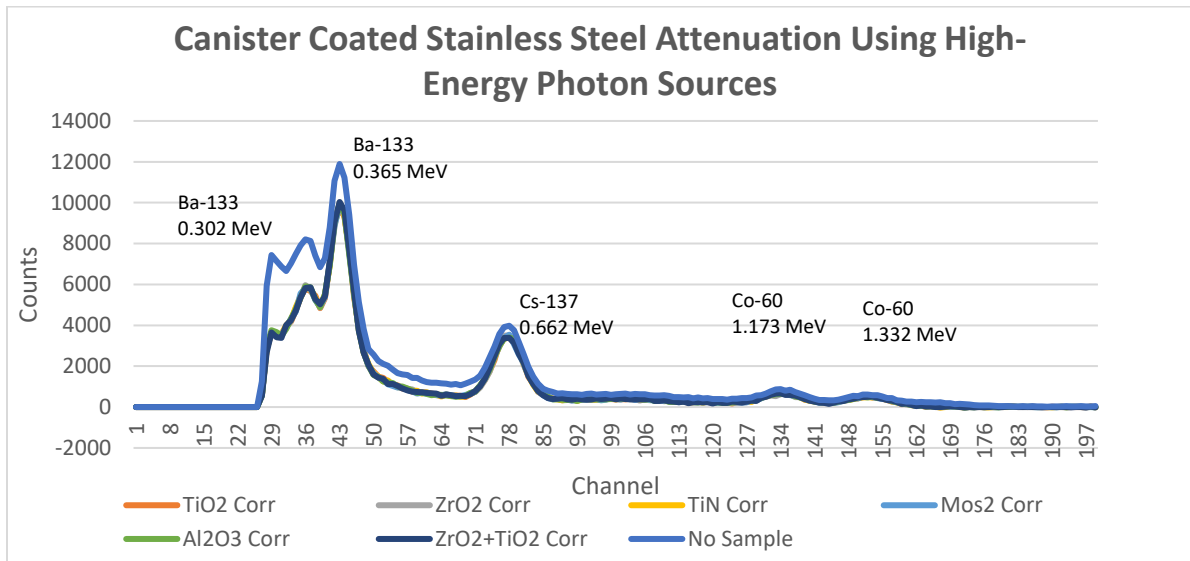


Figure 6. Measured counts of coated stainless steel substrates showing high-energy peaks.

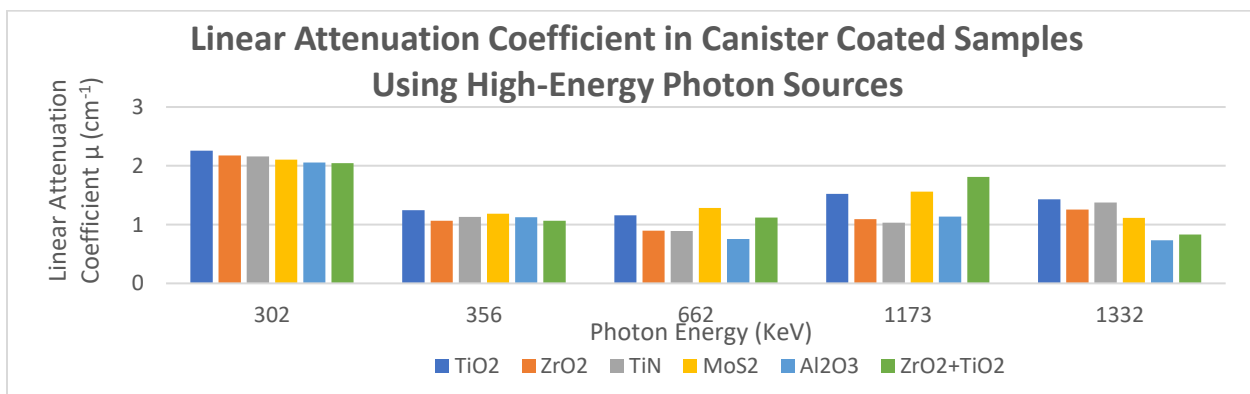


Figure 7. Determination of linear attenuation coefficients of various coatings on stainless steel substrates.

Computational modelling using MicroShield is performed to calculate the linear attenuation coefficient and half value layer of ZrO₂ and TiO₂ to compare the experimental results to computational modelling results. A strong correlation between experimental results and computational models is shown

in Figures 8 & 9. The calculated half value layers are close except in the case of a double layer on 316 SS where the HVL is slightly increased as shown in Figure 10.

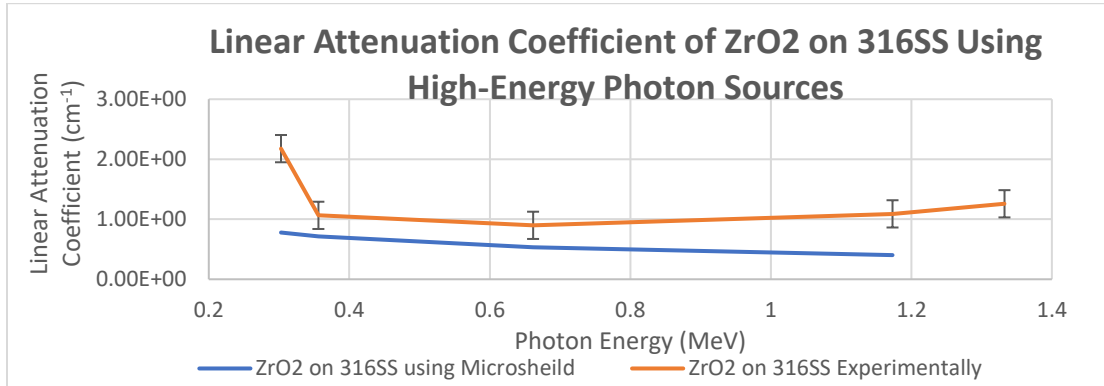


Figure 8. Comparison of experimentally and computationally calculated linear attenuation coefficients of ZrO_2 .

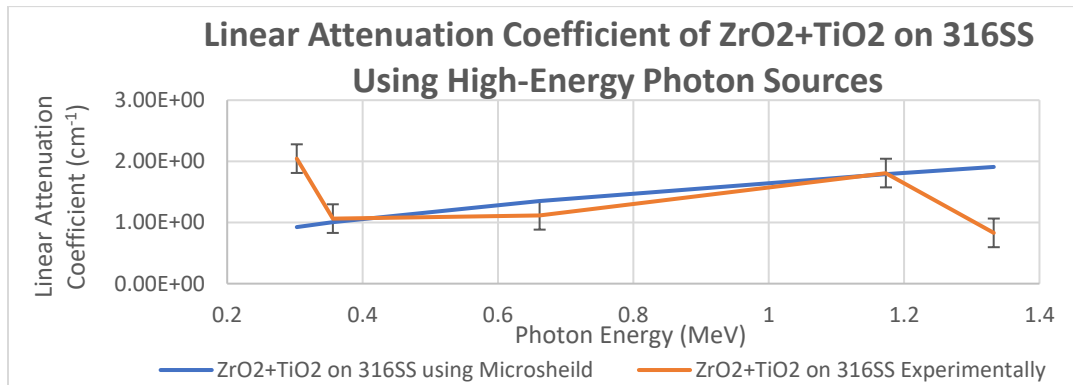


Figure 9. Comparison of experimentally and computationally calculated linear attenuation coefficients of multi-layered ZrO_2 and TiO_2 .

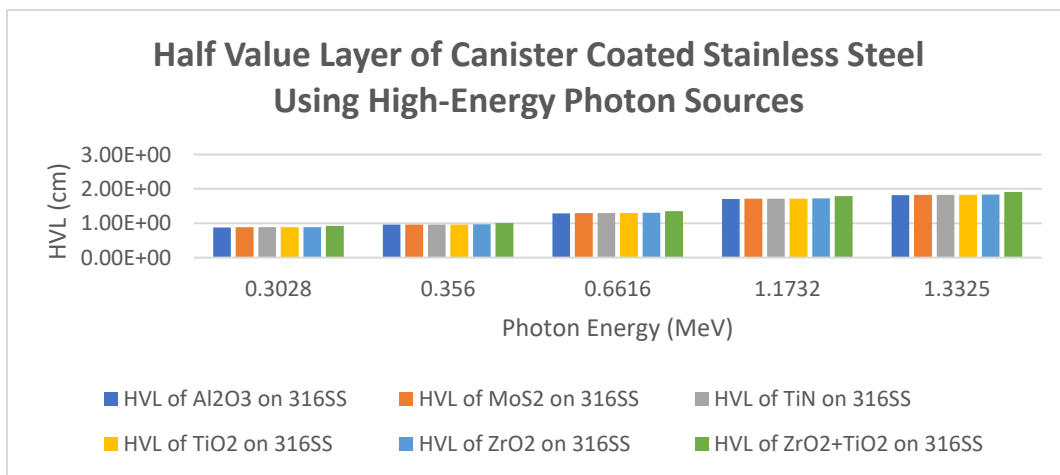


Figure 10. Determination of Half Value Layers of coated substrates on 316 SS.

Experiments and Modelling on Concrete

Similar experimental analysis is performed for concrete samples of various compositions and compared to simulated conditions using MicroShield software. Different mixtures of concrete are used, labelled Mix A and Mix B. Both mixtures have a composition of 50% special concrete, 25% boron, and 25% granite. The special concrete portion of Mixture A refers to a composition of 13.98% cement, 7.63% water, 10% lead, and the remaining filled with either granite, sand, or a half and half mixture of sand and granite.

The effect of concrete as a strong shielding material is shown in Figure 11. Samples of concrete mixtures with various compositions show slightly higher linear attenuation coefficients between 302 keV to 662 keV as seen in Figure 12.

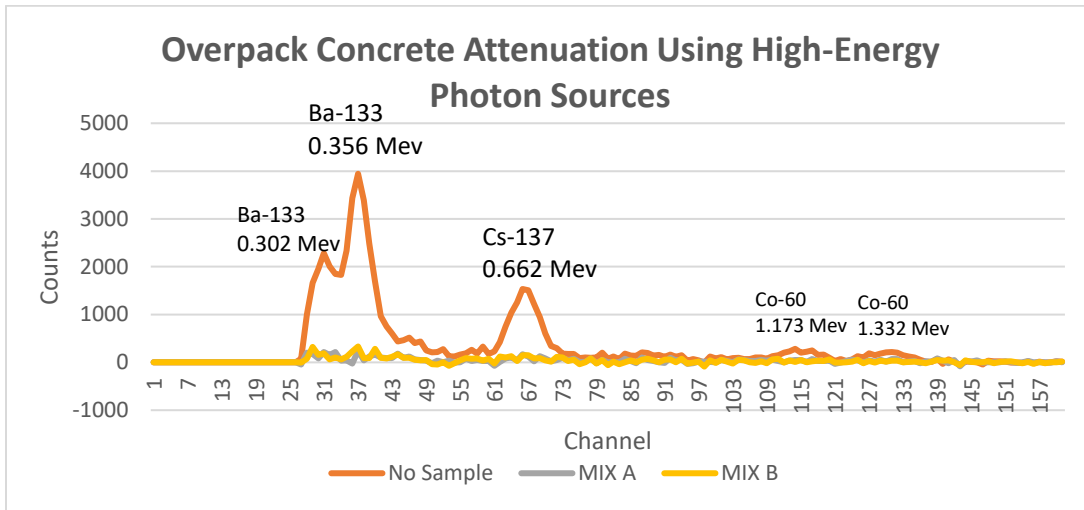


Figure 11. Measured counts of concrete samples of various mixtures showing high-energy peaks.

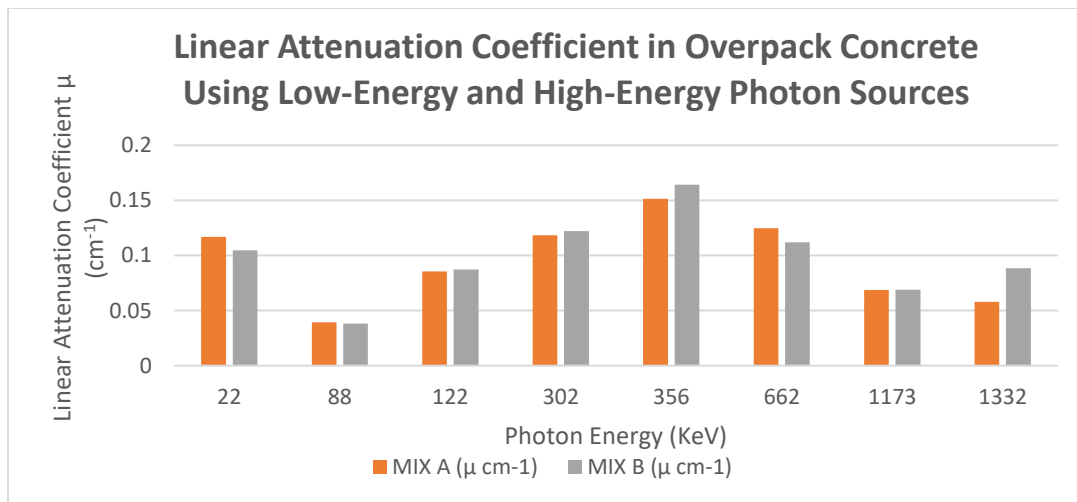


Figure 12. Determination of linear attenuation coefficients of two different mixtures of concrete overpack material.

Computational modelling using MicroShield is performed to calculate the linear attenuation coefficient and half value layer of concrete samples of Mixture A with sand and granite to compare the

experimental results to modelling results. A strong correlation between experimental results, literature values from Lamarsh and Baratta (2001), and computational models is shown in Figures 13 & 14 at high-energy values. The calculated half value layers are very close, thus not dependent on the choice of aggregate as shown in Figure 15.

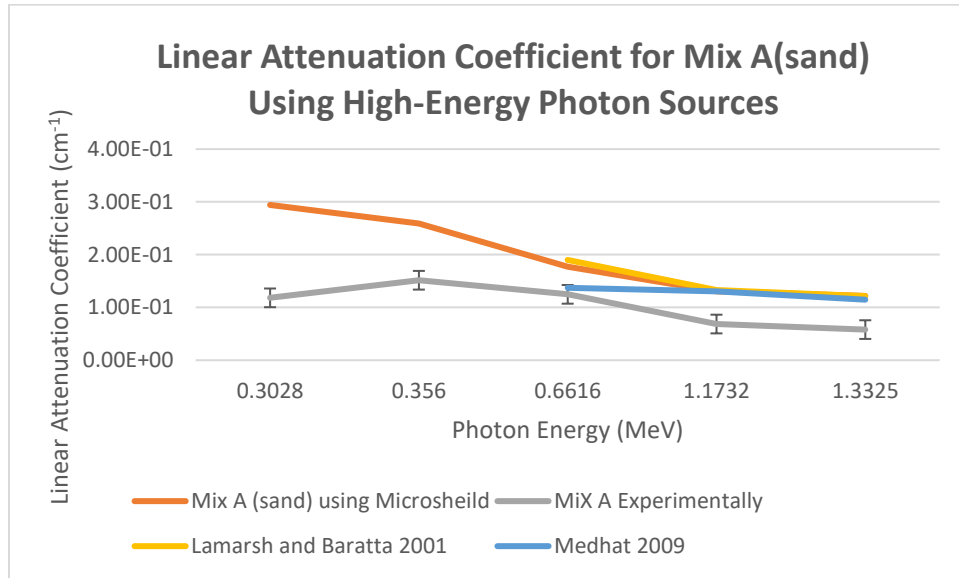


Figure 13. Comparison of experimentally and computationally calculated linear attenuation coefficients of Mixture A concrete with sand added using high-energy sources.

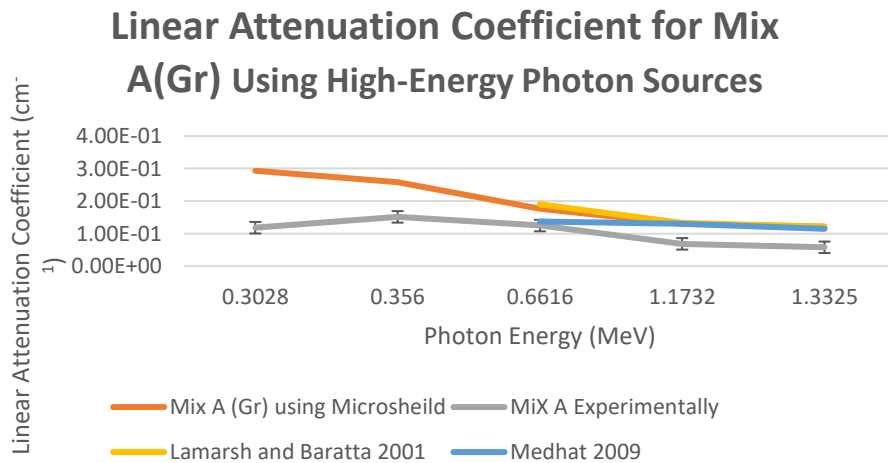


Figure 14. Comparison of experimentally and computationally calculated linear attenuation coefficients of Mixture A concrete with granite added using high-energy sources.

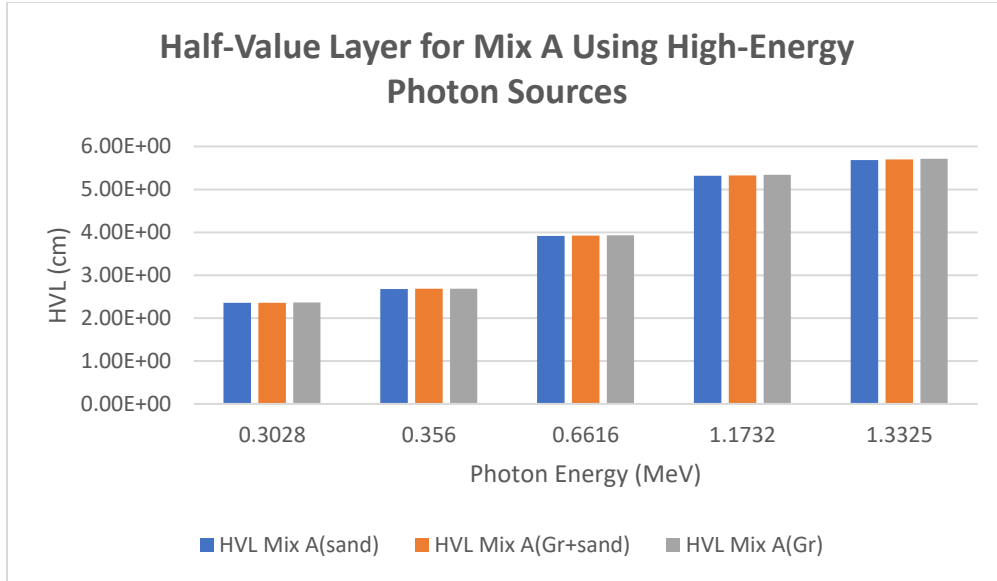


Figure 15. Determination of Half Value Layers of concrete Mixture A with various aggregates using high-energy sources.

The effect of concrete as a shielding barrier against low-energy sources is shown in Figure 16. Differences between the experimentally determined linear attenuation coefficient and the computationally determined linear attenuation coefficient are distinct at low-energies as seen in Figures 17 & 18. A poor correlation between the experimental and computational data occurs at energies below 88 keV. This is most likely due to the insufficient compositional data input into the MicroShield software. The calculated half value layers are very close, thus not dependent on the choice of aggregate as shown in Figure 19 at low-energies.

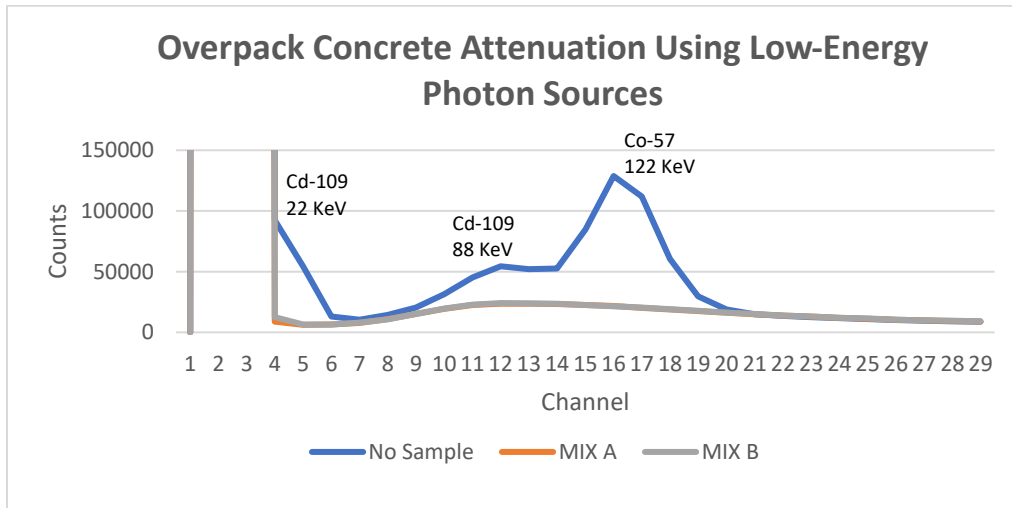


Figure 16. Measured counts of concrete samples of various mixtures showing low-energy peaks.

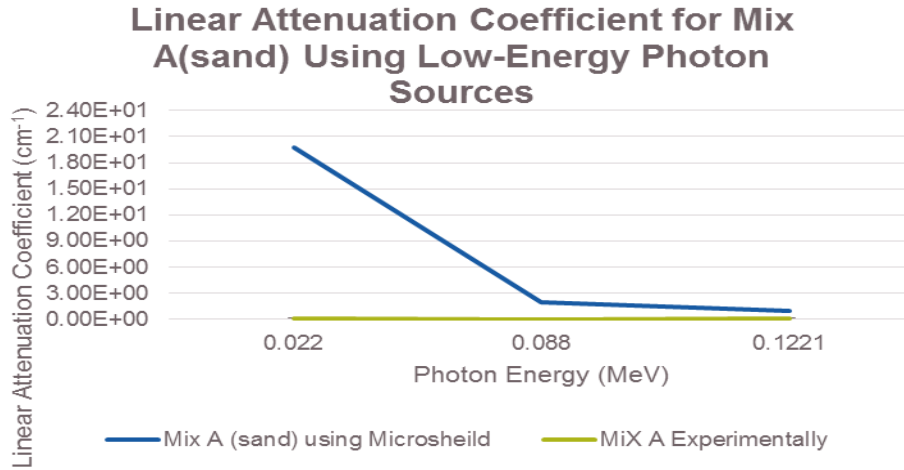


Figure 17. Comparison of experimentally and computationally calculated linear attenuation coefficients of Mixture A concrete with sand added using low-energy sources.

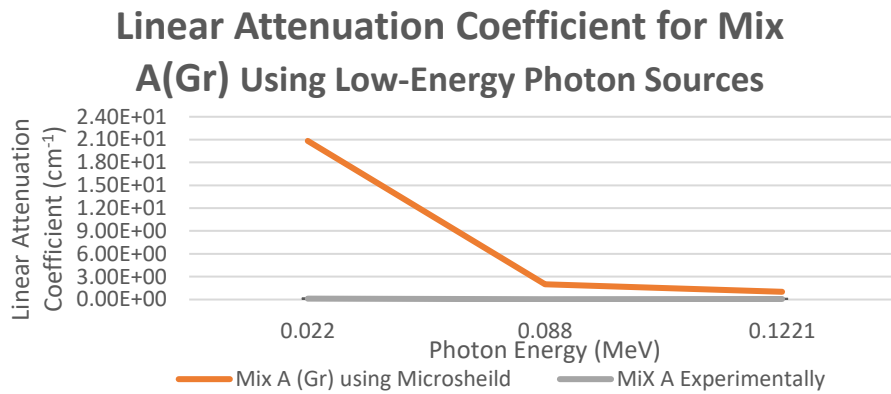


Figure 18. Comparison of experimentally and computationally calculated linear attenuation coefficients of Mixture A concrete with granite added using low-energy sources.

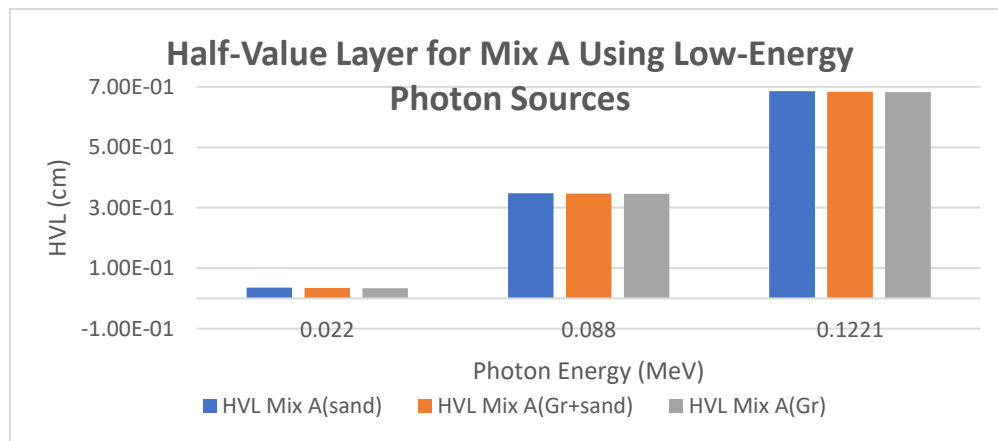


Figure 19. Determination of Half Value Layers of concrete Mixture A with various aggregates using low-energy sources.

Corrosion Testing

Single layer coated samples of MoS₂, ZrO₂, and TiN over a 40 day circulatory cycle show no significant mass loss from corrosion. The maximum change in mass over the 40 day period is calculated to be a 0.65% change. Stainless steel materials are known for their strong corrosion resistance, thus it is expected that over a short time period, no corrosion degradation is observed.

CONCLUSION

Thin film coatings provide sufficient corrosion resistance to stainless steels used in nuclear waste storage applications. The material coatings show slight variations in the linear attenuation coefficient at higher energies, thus the chosen material as the coating is important. The experimentally determined linear attenuation coefficient values for coated stainless steel substrates show good correlation to computationally generated values. Experimentally determined linear attenuation coefficients of concrete mixtures under high-energy sources show agreement with computationally determined values. The half value layer does not depend on the type of filler aggregate used. Under low-energy sources, the experimental and computational linear attenuation coefficients show differing values likely due to the limitation in modelling the composition of the concrete mixtures within the modelling software. Once again, the half value layer does not depend on the type of aggregate added at low energies. Both thin films and various mixtures of concretes prove to be effective shielding barriers, thus various thin film coatings and concrete mixtures should be used for long-term storage of spent nuclear fuel.

REFERENCES

- Kwon, Se-Hun, et al. "Plasma-Enhanced Atomic Layer Deposition of Ru-TiN Thin Films for Copper Diffusion Barrier Metals." *Journal of The Electrochemical Society*, vol. 153, no. 6, 2006, doi:10.1149/1.2193335.
- Lamarsh, John R., and Anthony John Baratta. *Introduction to Nuclear Engineering*. Pearson Education, Inc., 2001.
- Shan, C.x., et al. "Corrosion Resistance of TiO₂ Films Grown on Stainless Steel by Atomic Layer Deposition." *Surface and Coatings Technology*, vol. 202, no. 11, 2008, pp. 2399–2402., doi:10.1016/j.surfcoat.2007.08.066.
- Singh, H., et al. "An Investigation of Material and Tribological Properties of Sb₂O₃/Au-Doped MoS₂ Solid Lubricant Films under Sliding and Rolling Contact in Different Environments." *Surface and Coatings Technology*, vol. 284, 2015, pp. 281–289., doi:10.1016/j.surfcoat.2015.05.049.